A Miniaturized Loran H-field Antenna for Handheld Devices

David S. De Lorenzo, Sherman C. Lo, Morris Cohen, Jeff Chang,
Umran S. Inan, Per K. Enge (Stanford University)

Abstract

This paper presents Loran signal processing results for a series of successively smaller H-field square-loop antennas input to a preliminary design of low-noise-optimized, low-frequency ASIC. Antennas as small as 5cm (2-inches) on a side are able to detect Loran signals both outdoors and indoors, although in some cases significantly attenuated compared to signals from a larger 50cm (20-inch) antenna. Future work is aimed at developing a fully optimized LNA/ASIC design for the Loran frequency band at 100 kHz, in order to permit Loran operation with H-field antennas smaller than 1-inch (2.5cm).

Introduction

Loran position, navigation, and time (PNT) are desirable features in next-generation personal navigation devices (Figure 1). First, Loran can improve navigation accuracy and

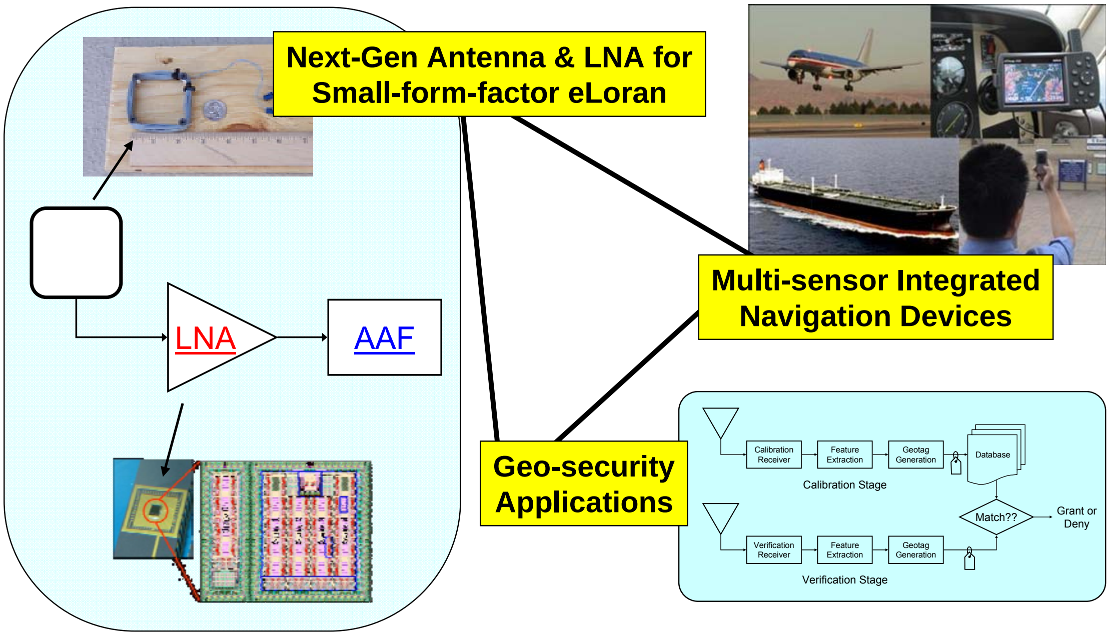

Figure 1. Enabling a Small Loran Antenna for Integrated Navigation Devices.

availability through multi-sensor integration [Doty *et al.*, 2003]. Second, Loran can enhance geo-security through its jam- and spoof-resistant signal characteristics of high transmit power and low carrier frequency [Qiu, 2007].

However, a major obstacle to the adoption of Loran navigation in mass-market handheld consumer electronics devices is the large size of the receiving antenna. Large antennas are needed in order to avoid excessive power loss due to the 3km wavelength of the 100 kHz Loran radio frequency (RF) carrier. This flies in the face of industry trends to reduce the size, weight, and cost of portable electronics, even at a time when navigation and location-based services are perceived as critical platform and vendor differentiators.

Shrinking the Loran antenna reduces the received signal strength and makes detection and feature extraction problematic [Lee *et al.*, 2009]. At a constant internal noise power, this limits the minimum realizable antenna size required to achieve acceptable signal-to-noise ratio (SNR). The approach pursued in this research is to combat the internal noise issue by focusing on the low-noise amplifier (LNA), and to trade improvements in internal noise power against smaller Loran H-field receive antennas.

This paper presents Loran signal processing results for a series of successively smaller H-field square-loop antennas input to a preliminary design of low-noise-optimized, low-frequency ASIC (application-specific integrated circuit). Antennas as small as 5cm (2-inches) on a side are able to detect Loran signals both outdoors and indoors, although in some cases significantly attenuated compared to signals from a larger 50cm (20-inch) antenna. Future work is aimed at developing a fully optimized LNA/ASIC design for the Loran frequency band at 100 kHz, in order to permit Loran operation with H-field antennas smaller than 1-inch (2.5cm).

Low-Noise Amplifier

The LNA developed and tested for this research is a preliminary design that has been integrated with extant low-frequency (ELF/VLF) radio reception and signal conditioning hardware. That system previously has been deployed for studies of atmospheric physics including remote sensing of lightning, ionosphere and magnetosphere characterization, and terrestrial and space-based radio propagation experiments [Cohen *et al.*, 2010; Harriman *et al.*, 2010]. To date, more than 50 systems employing this basic architecture have been fabricated.

Figure 2 shows the specifications of a single-chip LNA and AAF (anti-aliasing filter) design similar in concept to the discrete component implementation utilized herein. Characterization and analysis of the single-chip design was undertaken to evaluate whether the noise performance of the ELF/VLF hardware was likely to compensate for poor signal reception of reduced form-factor antennas.

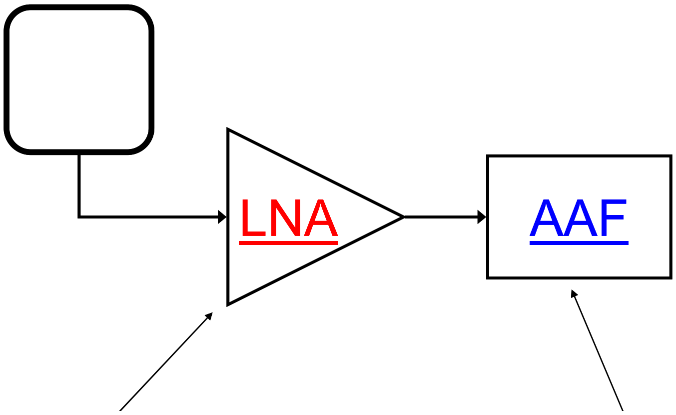

LNA Key Specifications

Adjustable Gain	0-20 dB
Bandwidth	100 Hz – 1 MHz
Input-referred Noise	10 nV/m/Hz½
Input Impedance	1 GΩ ‖ 100 fF
SFDR	100 dB

AAF Key Specifications

Architecture	6th-order Chebyshev (Type I)
Adjustable 3-dB Bandwidth	30 kHz, 180 kHz, 1080 kHz
Stopband Attenuation	-80 dB (3^*f_c), -96 dB (4^*f_c)
SFDR	100 dB
Power	70 mW

Figure 2. A very low-noise, low-power, high-linearity, wide-bandwidth, high-impedance LNA developed by Stanford EE STAR-Lab; the specifications are for a single-chip integrated device similar to the discrete component implementation utilized herein.

The single-chip LNA design exhibits a flat passband up to 100 kHz, accurate gain steps from 14 to 20 dB, and negligible flicker noise above 100 Hz. While linear gain is achieved for a 100 kHz input tone, the performance of this generation LNA does degrade above 100 kHz; this impacts reception of Loran signals which are centered at 100 kHz but extend also some 10+ kHz higher in frequency.

An input referenced noise value of $0.5\,\mu V/\sqrt{Hz}$ combined with an LNA bandwidth of 200 kHz yields an internal noise of approximately 220 µV:

$$0.50\,\mu V/\sqrt{Hz} \quad \times \quad \sqrt{200\,kHz} \quad \cong \quad 220\,\mu V$$

Eq. 1

Based on a 0.05m antenna effective height, this would yield an equivalent noise strength of $36.5\,dB\;\mu V/m$:

$$220\;\mu V/0.05\,m \quad = \quad 4.4\,mV/m \quad = \quad 36.5\,dB\;\mu V/m$$

Eq. 2

This equivalent noise strength can be compared to the expected Loran field strength of $\sim 30-110\,dB\;\mu V/m$ (assuming ~1500 km range to the transmitter), as well as to atmospheric noise of $\sim 45-60\,dB\;\mu V/m$. This indicates that it should be feasible to operate a usefully small Loran H-field antenna with this baseline LNA performance.

Antenna Designs

A sequence of successively smaller air-core H-field square-loop antennas was tested in both outdoor and indoor environments. While the air-core design was chosen for this preliminary study, it is possible that implementing antennas with dielectric cores could enable improved performance or allow further reduction in antenna size, however at a negative cost tradeoff. Antenna specifications are as indicated below in Table 1.

Table 1. Loran H-field Antenna Evolution.

Parameter	**Gen-1**	**Gen-2**	**Gen-3**	**Gen-4 (tbd)**
Antenna size	50cm	10cm	5cm	2.5cm
Wire gage	22 AWG	26 AWG	26 AWG	26 AWG
# of turns	9	19	37	74
Inductance	0.16 mH	0.10 mH	0.13 mH	0.23 mH
Resistance	1 Ω			

The H-field antennas were integrated with the LNA module and line receiver support electronics as indicated in Figure 3. The grey aluminum box contains the preamplifier and filtering circuits; the red case is the line receiver [Cohen *et al.*, 2010].

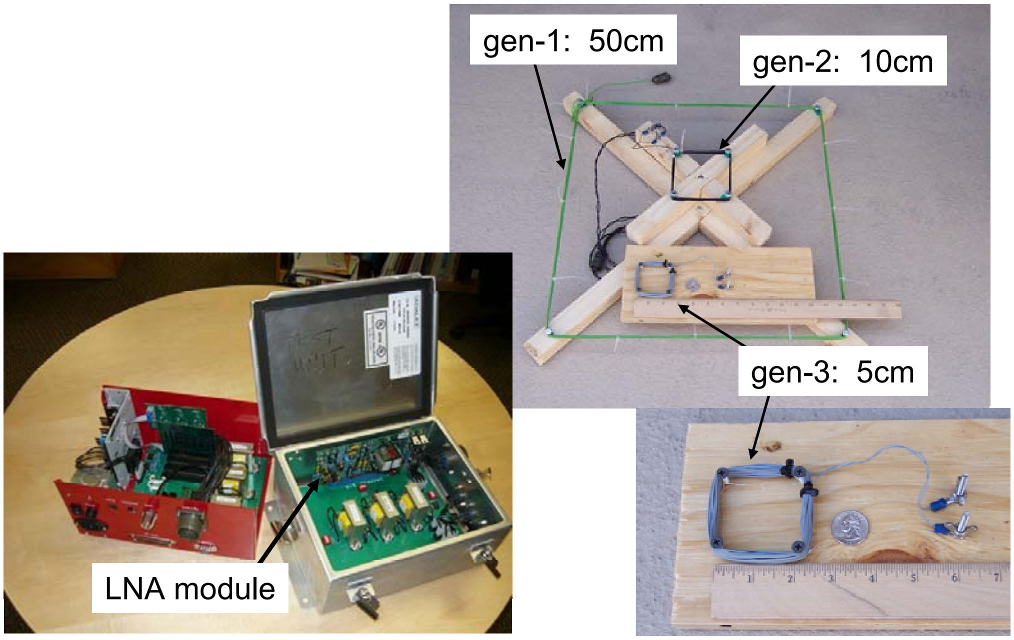

Figure 3. ELF/VLF radio reception system with various small-form-factor Loran antennas.

Experimental Results

The data collection equipment included H-field Loran antennas, optimized RF hardware, and an Agilent 89600 Vector Signal Analyzer (VSA) which digitized the signals and stored them for post-processing. Sampling locations were on the Stanford University campus, outdoors on the roof of the Durand Building and indoors in a 4th floor meeting area; the building construction is steel-reinforced concrete. Subsequent to data capture in outdoor and indoor locations, the signals were processed with a Loran software receiver implemented in Matlab. The experimental set-up is indicated in Figure 4.

Northern California is well-served by the Loran West Coast Chain (GRI-9940), with the Master Station 360km distant in Fallon, NV, and Secondary Stations in George, WA, Middletown, CA, and Searchlight, NV; the most-distant secondary is George at approximately 1100km distant.

With the 50cm (20-inch) H-field antenna, the signal pulse sequences are readily visible in the time domain, as shown in Figure 5 – no averaging is required, and changing the orientation of the antenna will reveal the signal direction-of-arrival (DOA). As the antenna size gets smaller, the signal strength reduces as well, as shown in Figure 6.

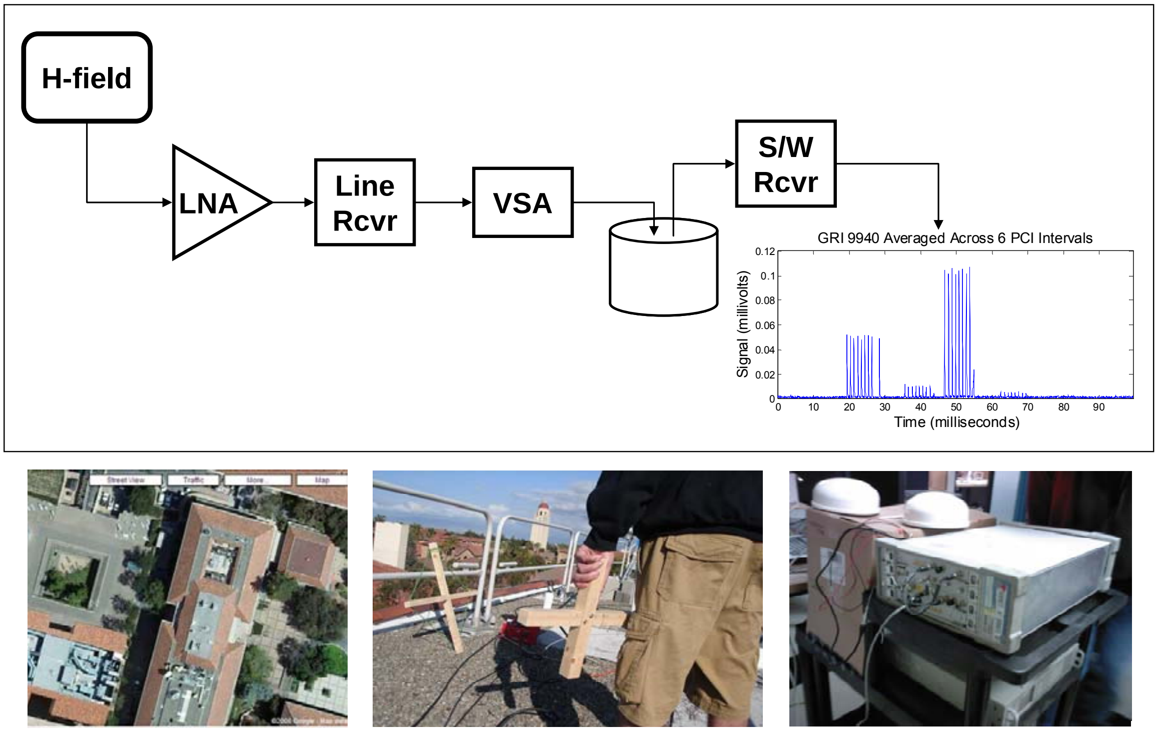

Durand Building, Stanford University

Outdoor data collection site

Agilent Vector Signal Analyzer

Figure 4. Loran data collection set-up.

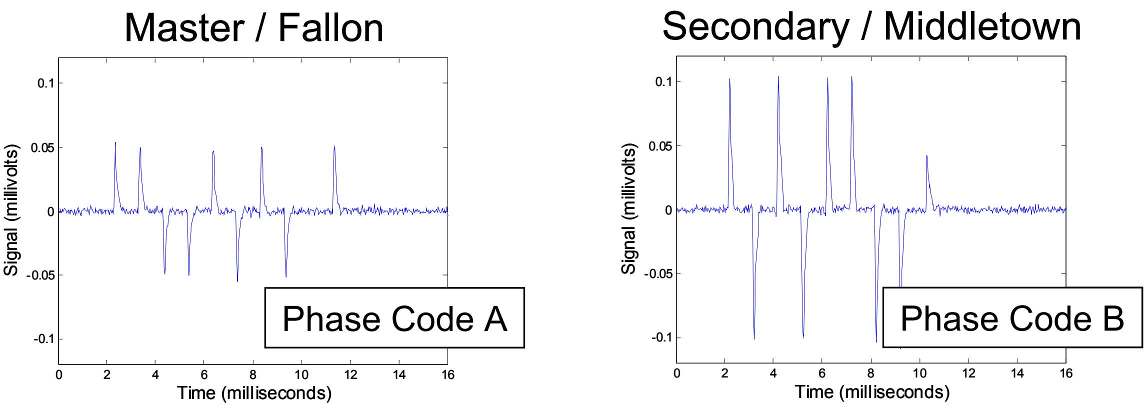

Master / Fallon

Secondary / Middletown

Figure 5. Loran signals from proximate stations – Fallon/Master and Middletown/Secondary – and 50cm H-field loop antenna.

Outdoor Data Collection – Palo Alto, CA

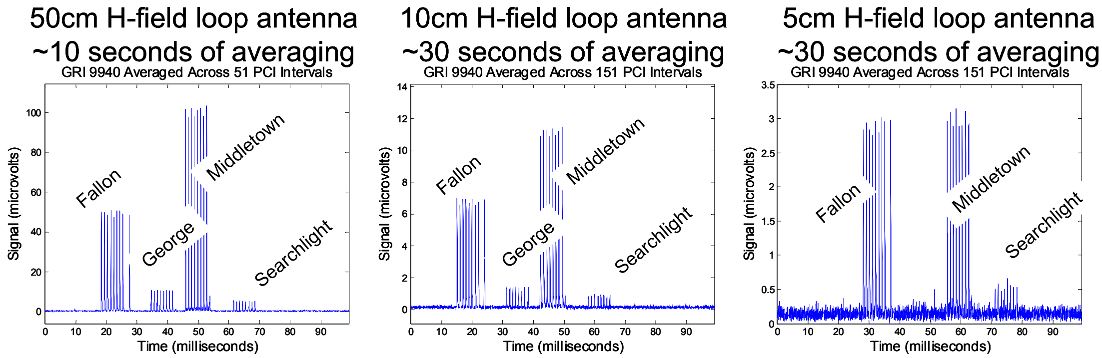

50cm H-field loop antenna ~10 seconds of averaging

GRI 9940 Averaged Across 51 PCI Intervals

10cm H-field loop antenna ~30 seconds of averaging

GRI 9940 Averaged Across 151 PCI Intervals

5cm H-field loop antenna ~30 seconds of averaging

GRI 9940 Averaged Across 151 PCI Intervals

Indoor Data Collection – Reinforced Concrete Multi-story Building

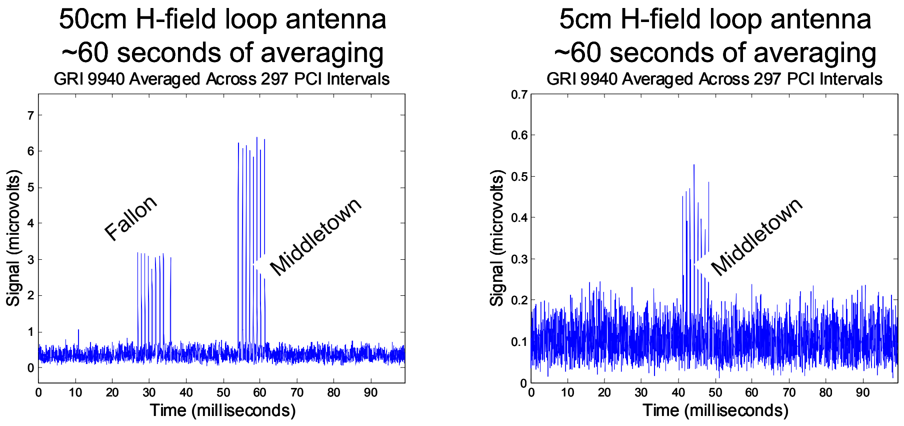

50cm H-field loop antenna ~60 seconds of averaging

GRI 9940 Averaged Across 297 PCI Intervals

5cm H-field loop antenna ~60 seconds of averaging

GRI 9940 Averaged Across 297 PCI Intervals

Figure 6. Loran West Coast Chain as observed from Palo Alto, CA.

For the outdoor data collection, the large antennas (50cm and 10cm) easily process the available signals, although the 5cm loop antenna requires fairly long averaging times to bring the signal above the noise. For the indoor data collection, signal attenuation is severe in the reinforced concrete building chosen for these tests; Fallon and Middletown are detectable after 60 seconds of averaging for the 50cm antenna, however only Middletown is detectable after 60 seconds of averaging for the 5cm antenna. The received signal strength for the Loran stations on the U.S. West Coast Chain are summarized in Table 2.

Table 2. Loran received signal strength (μV).
U.S. West Coast chain observed from Palo Alto, CA

Station	**Dist. (km)**	**Outdoors**			**Indoors**	
		50cm	**10cm**	**5cm**	**50cm**	**5cm**
Fallon	360	50	6.8	2.9	3.1	-
George	1,100	14	2.1	0.5	-	-
Middletown	160	210	27.1	17	7	0.46
Searchlight	680	8.5	1.3	0.9	-	-

Projection with Improved LNA Design

Projections of a further evolution of this baseline LNA design promise improved performance, primarily by limiting signal bandwidth prior to digitization. Reducing the bandwidth from 200 kHz to ~20 kHz by inclusion of a band-pass or high-pass filter will improve the internal noise to approximately $31\,dB\ \mu V/m$:

$$0.50\,\mu V/\sqrt{Hz} \quad \times \quad \sqrt{20\,kHz} \quad \cong \quad 70\,\mu V \qquad \text{Eq. 3}$$

$$70\ \mu V/0.05\,m \quad = \quad 1.4\,mV/m \quad = \quad 31\,dB\ \mu V/m \qquad \text{Eq. 4}$$

With this improved LNA design, we anticipate successful detection with H-field loop antennas smaller than 5cm (2-inches) square (Figure 7). We anticipate sufficient SNR to resolve time-difference of arrival (TDOA) and to achieve a position fix, although at reduced accuracy compared to systems employing larger receive antennas.

Conclusions

In this study, we have shown that reducing antenna size should focus ideally on internal noise, and that improved LNA design allows a trade of internal noise against antenna

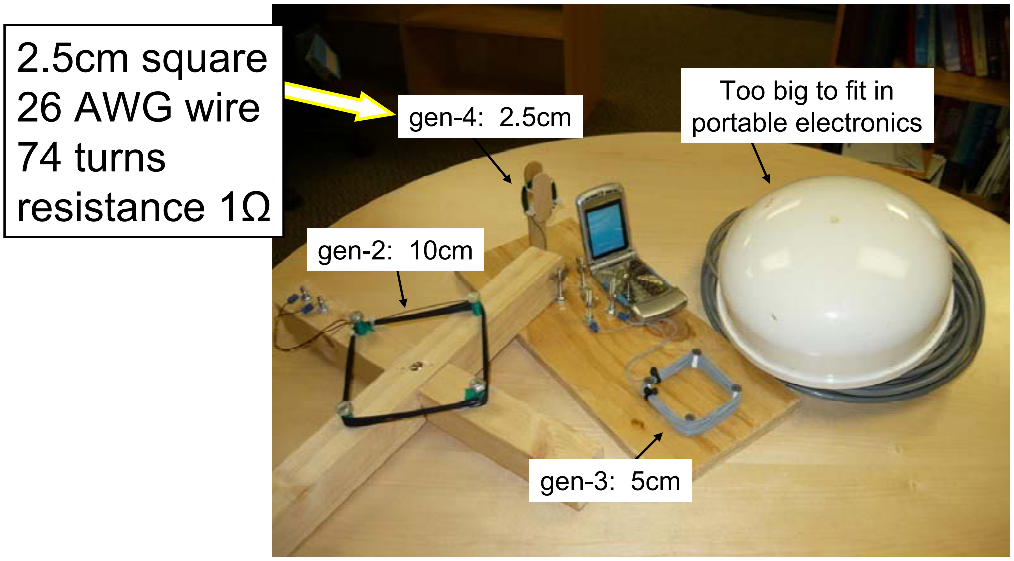

Figure 7. Next generation antenna design:
2.5cm air-core H-field antenna.

sensitivity. While long averaging times were required to combat low SNR, the Loran signals were detectable both outdoors and indoors with the smallest antenna size tested, namely a 5cm (2-inch) H-field air-core loop antenna. While timing and data services are enabled, due to limited station observability indoor navigation is not yet achieved with this LNA design, likely due to the excessive attenuation in reinforced concrete buildings. Current analysis suggests improved performance with a further optimized LNA, suggesting that a next-generation H-field air-core antenna of 2.5cm (1-inch) would be enabled.

Acknowledgements

The authors would like to thank Mitch Narins of the FAA Loran Program Office for supporting this work.

References

[1] M.B. Cohen, U.S. Inan, and E.W. Paschal, 2010, "Sensitive Broadband ELF/VLF Radio Reception with the AWESOME Instrument," *IEEE Trans. Geosc. Remote Sensing*, vol. 48, no. 1, pgs. 3-17.

[2] J.H. Doty, P.Y. Hwang, G.L. Roth, and M.J. Narins, 2003, "Integrated GPS/Loran Navigation Sensor for Aviation Applications," *Proc. ION GPS/GNSS*, pgs. 470-479.

[3] S.K. Harriman, E.W. Paschal, and U.S. Inan, 2010, “Magnetic Sensor Design for Femtotesla Low-Frequency Signals,” *IEEE Trans. Geosc. Remote Sensing*, vol. 48, no. 1, pgs. 396-402.

[4] D. Lee, S. Best, D. Hanna, and E. Rosario, 2009, “A Miniature LORAN H-Field Antenna for Low-Profile Conformal Hybrid Applications,” *Proc. ION Intl. Technical Meeting*, pgs. 869-874.

[5] D. Qiu, 2007, “Security Analysis of Geoencryption: A Case Study Using Loran,” *Proc. ION GNSS*, pgs. 1146-1154.